Shedding Light on DNA Analysis

Multiplexed Detection and Identification Using Fluorescence Lifetime Methods

Suzanne J. Lassiter, Wieslaw J. Stryjewski, Yun Wang, and Steven A. Soper*

*To whom all correspondence should be addressed

Continued efforts are being invested into further enhancing technologies directed toward analyzing genomes for both sequencing and diagnostic applications. One of the major focus areas is improving multiplexing capabilities to increase the information content available in a single assay. To this end, several research groups are focused on developing fluorescence time- and phase-resolved techniques to identify unique reporters through their intrinsic fluorescence lifetimes. This article provides a review of using both time- and phase-resolved fluorescence for DNA analysis for both sequencing and microarray applications.

The massive efforts invested in the Human Genome Project have begun to wind down as the final sections of the genome's sequence are being filled (1,2). However, a need still exists for higher throughput and more accurate DNA sequencing methods for the analysis of other organisms' genomes, comparative sequencing, gene therapy, or gene discovery endeavors.

To analyze DNA, it must be amplified and labeled with a fluorescent dye that can be identified readily. Through a method called *Sanger sequencing*, deoxynucleotides — the four base units in DNA (adenine, guanine, thymine, and cytosine) — form a complement to the template DNA molecule until a dideoxynucleotide incorporates and terminates the extension process. This extension and termination occurs multiple times and forms all possible fragment lengths of the template DNA molecule, which must be size sorted, typically using electrophoresis.

The use of fluorescence detection in DNA analyses has become the preferred method because it can provide on-line analysis and low limits of detection, as well as allow base-calling to be performed in one separation lane using multiplexed detection. In most DNA sequencing applications, four spectrally distinct reporters — one for each nucleotide base — are attached to either a sequencing primer or dideoxynucleotide and identified by their unique emission maxima. Although successful, the use of spectral discrimination techniques can create potential difficulties, including the need for multiple excitation sources and detection channels, cross-talk between detection channels, and dye-dependent electrophoretic mobilities of the labeled oligonucleotides. However, energy-transfer dye systems have relaxed some of these shortcomings for multiplexed DNA assays using color discrimination because it requires the use of only one excitation source (3).

Three main platforms can be used to size separate DNA fragments. The first is slab gel electrophoresis, which requires crosslinked polyacrylamide or agarose gel to fractionate DNA and may take 5–12 h for complete separation. The gel setup consumes liters of buffer and microliters of samples, but as many as 96 samples can run in parallel. The second platform is capillary gel electrophoresis, which

usually is performed in fused silica tubes, requires milliliters of buffer and nanoliters of sample for separations, and can be completed in 1–4 h. A number of gel-separation matrices can be used to perform the separation in capillary electrophoresis, including crosslinked polyacrylamides, linear poly- and polydimethylacrylamides, hydroxyethyl cellulose, and methylcellulose. Finally, microchip electrophoresis formats complete separations in 20–60 min and consume microliters of buffer and picoliters of sample. These chips are made using a variety of lithographic techniques in various types of materials, such as glass or polymers. Clearly, new separation platforms have tremendously reduced the development time on the electrophoresis — thereby increasing system throughput — but at the same time, have placed heavy demands on the readout mode because of reductions in the amount of sample loaded.

Recently, several groups have been investigating the use of fluorescence lifetimes to identify nucleotide bases. One of the primary limitations of spectral identification techniques is the broad emission profiles associated with molecular systems. As such, only a limited number of probes can be processed simultaneously. To increase multiplexing capabilities, additional fluorescence probes are required, such as those possessing unique fluorescence lifetimes. The fluorescence lifetime τ_f is an intrinsic photophysical parameter of chromophores and is a measurement of the average time difference between electronic excitation and fluorescence emission. The advantages of using lifetime analysis are that only one excitation source and detector might be required, the calculated lifetime is immune to concentration differences, the fluorescence lifetime potentially can be determined with high precision, and the technique can increase the information content within a sample to improve the accuracy of identification. In addition, lifetime methods, when coupled with color discrimination, can increase multiplexing capabilities.

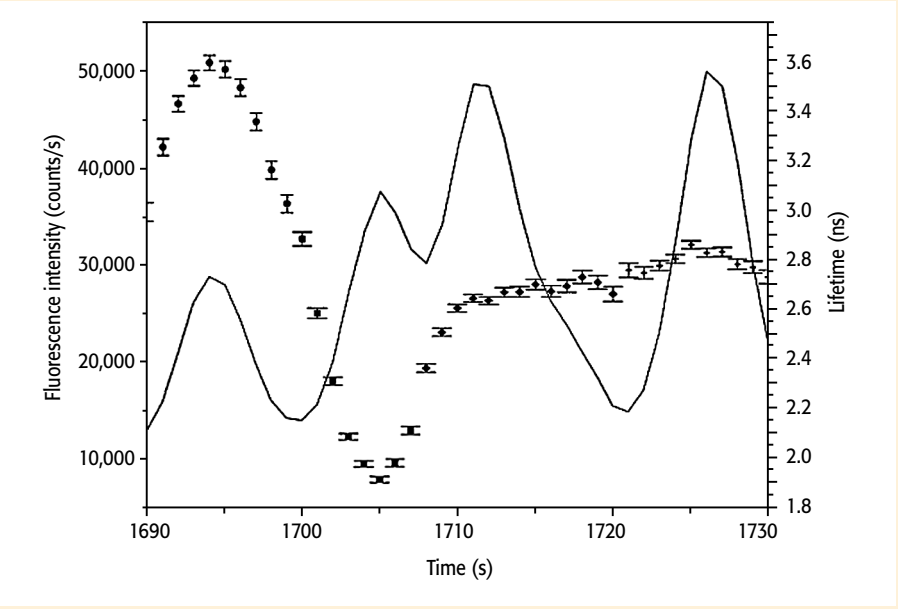

Figure 1. Electropherogram (solid line), fluorescence decay times (symbols), and errors (standard deviations in the decay time determination) of a small part of a sequencing run to illustrate the lifetime distribution inside and between peaks. Reprinted with permission from reference 7.

Lifetime calculations can be performed using either time- or phase-resolved methods. The time-domain method requires pulsed excitation to generate a decay curve, from which the fluorescence lifetime is calculated. Specifically, a high-repetition-rate pulsed laser is used to excite the sample, and the time difference between the exciting laser pulse and detection of the fluorescence photon is measured electronically. The measurement is repeated many times, with the time differences histogrammed to construct the decay profile. In most time-domain measurements, the shortest lifetime that can be measured reliably is determined by the response time of the instrument (referred to as the instrument response function [IRF]), which depends on the width of the excitation pulse, the spread of the travel times of photoelectrons in the photon detector, and the jitter in the measuring electronics. The IRF can be deconvolved (removed from the decay) using deconvolution algorithms to pro-

Table I. Accuracy of base identification using a monoexponential maximum likelihood estimator (MLE) algorithm and pattern recognition technique*

		Base number					
		51–150	151–250	251–350	351–450	451–550	551–660
MLE	Identification accuracy	91.0%	91.6%	82.4%	79.4%	60.4%	54.7%
	Overall identification accuracy	91.0%	91.3%	88.5%	86.6%	83.2%	80.0%
Pattern recognition	Identification accuracy	93.0%	95.8%	87.9%	86.3%	86.8%	88.7%
	Overall identification accuracy	93.0%	94.4%	92.3%	91.1%	90.5%	90.3%

*Adapted from reference 7. Identification accuracy is given for base calls in the base range listed for each column. Overall identification accuracy is a cumulative accuracy from beginning of base call (base 51) to the end base number listed in each column.

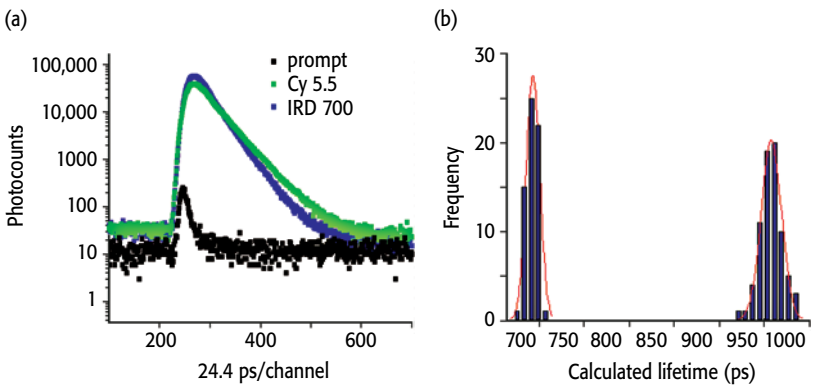

Figure 2. (a) Instrument response function and fluorescence decay profiles for IRD 700-labeled G sequencing fragments and Cy 5.5-labeled G sequencing fragments. (b) Histograms showing the fluorescence lifetimes calculated for IRD 700 and Cy 5.5 single-dye tracts of G sequencing ladders. Reprinted with permission from reference 8.

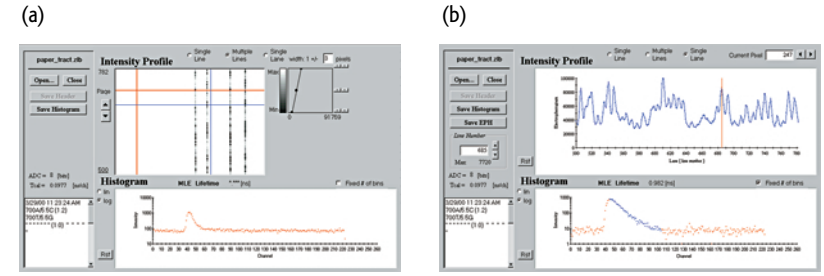

Figure 3. Display screens for data analysis. (a) Upper portion of screen shows slab gel intensity image of electrophoresis with instrument response function (IRF) on lower half of display. (b) Top portion of screen shows intensity electropherogram. Bottom portion displays selected decay profile and allows selection of time channels over which MLE will calculate lifetime.

vide a more accurate representation of the lifetime of the reporter.

The frequency domain incorporates a continuous wave source that is intensity modulated at a high frequency to produce a time-dependent intensity signal, which is composed of a sinusoidal wave superimposed on a time-independent intensity component. The fluorescent emission is phase shifted with respect to the light source and demodulated. The result is used to calculate the fluorescence lifetime. For phase-resolved measurements, the ability to measure short lifetimes depends on the frequency of the modulation and the efficiency of the phase-sensitive measuring electronics.

After the fluorescence decay of the reporters is collected, an analysis of the profiles is performed to calculate the fluorescence lifetime. A number of mathematical techniques can be used to calculate and evaluate the fluorescence lifetime, including nonlinear least-squares (NLLS) analysis, maximum likelihood estimator (MLE), or pattern recognition.

The goal of NLLS analysis is to obtain estimates of the parameters describing the decay and having the highest probability of being correct based on a starting model. The parameters that provide the best match between the data $N(t_k)$ and the calculated decay $N_c(t_k)$ are accepted on the basis of the minimization of the goodness of fit parameter χ^2 (4), in which χ^2 is calculated from

$$\chi^2 = \sum_{k=1}^{n} \frac{[N(t_k) - N_c(t_k)]^2}{\sigma_k^2} = \sum_{k=1}^{n} \frac{[N(t_k) - N_c(t_k)]^2}{N(t_k)} \quad [1]$$

The sum extends over n — the number of channels or data points used in the analysis. The value of σ_k is the standard deviation associated with each data point. In most NLLS analyses, the measured data are compared with values predicted from a model, and the parameters of the model are varied to yield the minimum deviations from the data. Two advantages of NLLS analysis are its ability to remove the contribution of the IRF through deconvolution, thereby increasing the accuracy in the determination, and that it allows multi-exponential decays to be analyzed.

The MLE can be used to calculate decay parameters for single-exponential functions using the following equation:

$$1 + (e^{\frac{T}{\tau}} - 1)^{-1} - m(e^{\frac{mT}{\tau}} - 1)^{-1} = N_t^{-1} \sum_{i=1}^{m} iN_i \quad [2]$$

in which T is the width of each channel, m the number of time channels, N is the total number of photon counts, N_i is the number of photon counts in time channel i, and τ is the calculated lifetime (5,6). In this algorithm, which does not perform a deconvolution, the variance in the calculated lifetime is low even when the number of photon counts is low. This equation is used to calculate only one lifetime from a decay, even in the case of multiexponential decays.

Identification of the labels also can be accomplished using pattern recognition, which has four major components: data acquisition and collection, feature extraction and representation, similarity detection and pattern classifier design, and performance evaluation. In the case of statistical regression, pattern recognition seeks an approximating function that minimizes the probability of misclassification. For evaluation of lifetime values using a pattern recognition technique, fluorescence decays are collected under conditions similar to the actual experimental conditions and serve as the patterns to compare with the experimental decays for lifetime identification.

Wolfrum and coworkers recently demonstrated multiplexed one-lane capillary sequencing using time-resolved fluorescence with a set of red dyes (7). Four dye labels selected from the rhodamine, cyanine, and oxazine families were covalently tethered to oligonucleotide primers and used in cycle sequencing. The dyes exhibited similar absorption and emission maxima and were excited efficiently with a 630-nm pulsed diode laser. To compensate for dye-dependent mobility shifts within the dye set, an 8-aminocaprylic acid linker was added between the dye and oligonucleotide of the faster migrating complex. In addition, concentrations of the four sequencing reactions were adjusted to give similar peak heights. Differences in fluorescence intensities resulted from different fluorescent quantum yields and extinction coefficients of the dyes at the monitoring wavelengths. The labels had lifetime values of 1.6, 2.4, 2.9, and 3.7 ns, adequate for efficient identification in gel sequencing runs (see Figure 1). The sequencing reactions were performed on an M13mp18 template and dye-labeled M13(−21) primers with electrophoretic size sorting using capillary gel electrophoresis.

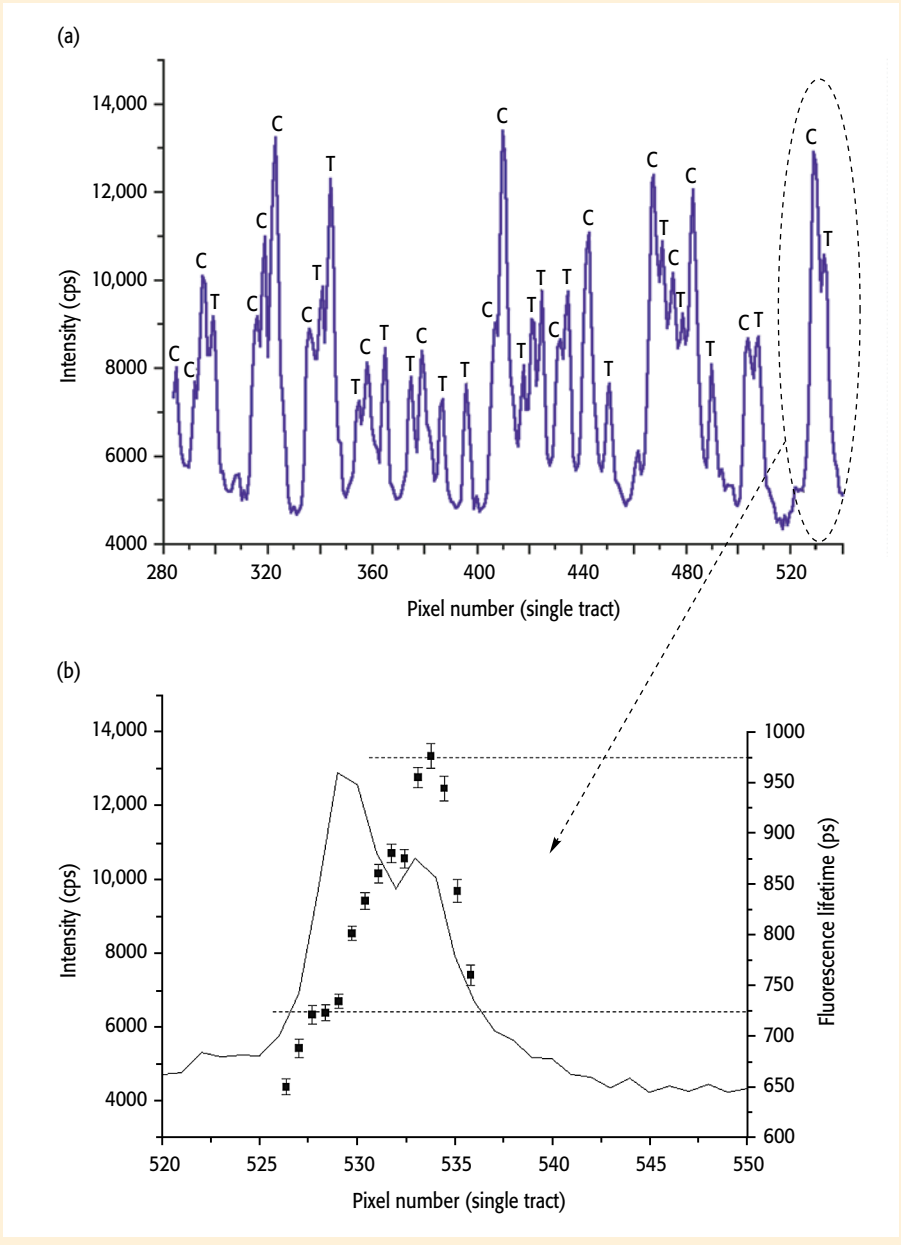

Figure 4. (a) Intensity electropherogram along with base-calling assignments obtained from the calculated lifetime. (b) Expanded view of bands from (a). The dashed lines represent expected lifetimes. Reprinted with permission from reference 8.

The 630-nm laser was pulsed with a self-matched tunable pulse generator operating at a repetition rate of 22 MHz. The instrument response function was 600 ps (fwhm). The beam was coupled to the capillary gel column by using a dichroic mirror and microscope objective. The fluorescence was collected by the same objective and imaged onto the active area of an avalanche photodiode that served as the photon transducer. Data acquisition was accomplished through a time-correlated, single-photon counting PC interface with the electronics card mounted on a PC bus. The fluorescence signal was collected with an integration time of 1 s, and as many as 60 decay profiles were collected per cycle and stored in memory.

The time-resolved data were used to create an electropherogram by accumu-

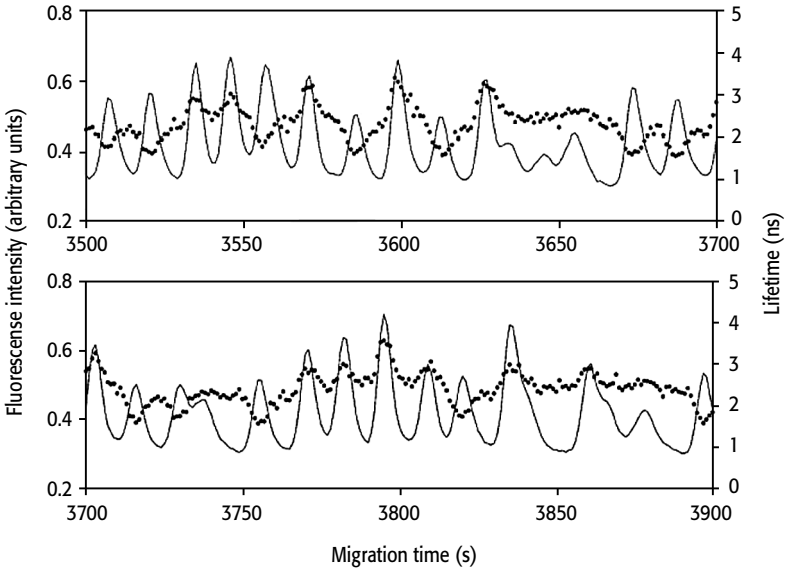

Figure 5. Section of fluorescence lifetime (dotted line) and intensity (solid line) electropherograms for four-decay sequencing. Reprinted with permission from reference 9.

lating all the photoevents of each decay into 1-s time intervals and plotting the values versus the migration time. The labeled sequencing fragments then were identified using MLE and pattern recognition. The authors found that the pattern recognition technique provided a higher overall base-calling accuracy, 90.3% for 660 base reads, compared with 80% accuracy using the MLE calculation for the same read length. (See Table I for a summary of results.) The lower accuracy of the MLE method was attributed to biexponential fluorescence decays produced from two dye bands overlapping, caused by poor electrophoretic peak resolution, which the MLE could not distinguish and treated as an average of the two components. Improving electrophoretic peak resolution would increase the accuracy of base identification using lifetime methods for both calculation methods, according to the authors.

The work by Wolfrum et al. demonstrated lifetime reading from a single capillary and a stationary detector. To show that scanning systems can be used to read fluorescence lifetimes from multiple electrophoretic lanes, Soper and coworkers constructed a compact, time-correlated, single-photon counting microscope that easily could be rastered over gels (8).

Multiple lanes in electrophoresis can be read by imaging the individual lanes onto an array detector or sequentially scanning the detector over the multiple lanes. Because imaging detectors with sufficiently small timing responses appropriate for time-resolved fluorescence do not exist, a scanner system was used. The scanner was constructed from a fluorescence microscope found in an automated slab gel instrument, which was modified by adding a pulsed diode laser and an actively quenched large photoactive area avalanche photodiode, giving a large dynamic range and favorable timing response (400 ps, fwhm).

The laser, operating at 680 nm, was mounted on the microscope head at a 56° angle with respect to the boro-float gel plates to minimize reflected radiation from being coupled into the optical system. The laser was driven by an electrical short-pulse generator, which supplied high-repetition-rate (80-MHz) picosecond current pulses to the diode head. One PC-based card situated in a computer contained all the electronics for time-correlated, single-photon counting and processing of the time-resolved data.

The data acquisition software was written in Visual Basic and consisted of several control and data acquisition functions such as recording the position of the scanning head, streaming intensity and time-resolved data to the hard drive, and providing real-time visualization of the acquired data.

The ability to identify a particular labeling dye comprising an electrophoretic band when more than one dye is present depends not only on the number of photons counted in the band but also on the electrophoretic resolution between bands because the MLE algorithm, which was used to determine the lifetimes, can extract only one value — even in cases in which a multiexponential decay exists. Therefore, the read length of the sequence trace will depend not only on the signal intensity in the bands but also on the ability to acquire a lifetime value where minimal band overlap occurs.

Two commercial dyes, IRD 700 and Cy 5.5, were chosen as labels for the oligonucleotide sequencing primers because of their similar absorption and emission properties that allow efficient processing on one detector channel. However, a post-electrophoresis base correction was needed because of the different charges on the molecules producing dye-dependent electrophoretic mobilities. These dyes were determined to have lifetime values of 718 $\pm$ 5 ps and 983 $\pm$ 13 ps, respectively, which were calculated over 65 bands from individual base tracts run in separate lanes of the gel (see Figure 2).

A two-dye/two-lane experiment was carried out with A (IRD 700) and T (Cy 5.5) tracts in one lane and C (IRD 700) and G (Cy 5.5) tracts in an adjacent lane. Figure 3 shows an intensity electropherogram and data analysis screen for this time-resolved fluorescence experiment. A four-lane read, with each base tract run in individual lanes, was carried out to directly compare the read length and accuracy of the MLE base identification method with those of the four-lane protocol. When bands significantly overlapped, a pixel-by-pixel analysis from the image was used to extract the lifetime value to improve read

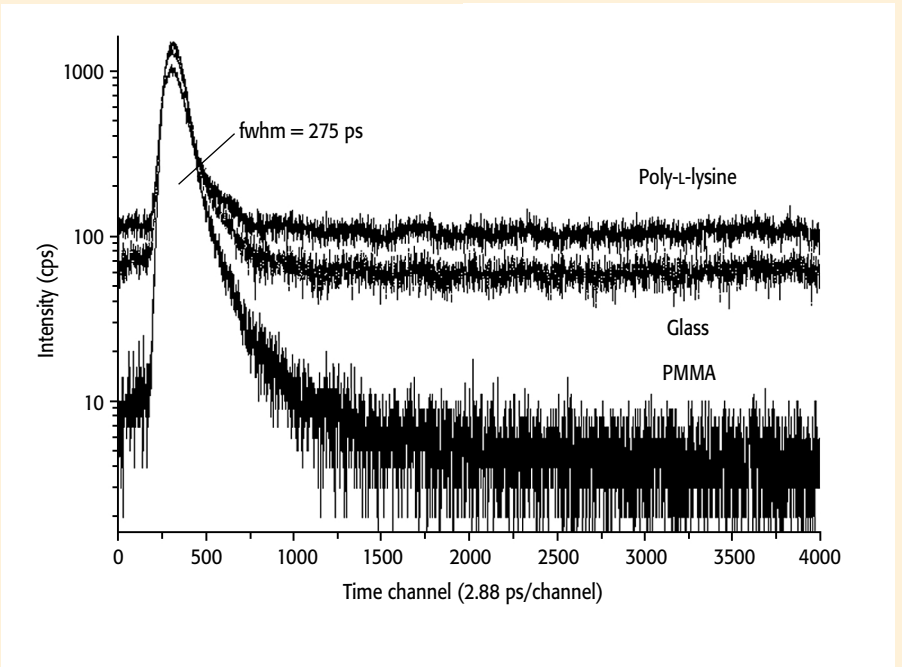

Figure 6. Decay profiles for glass, PMMA, and poly-L-lysine–coated slides. Reprinted with permission from reference 10.

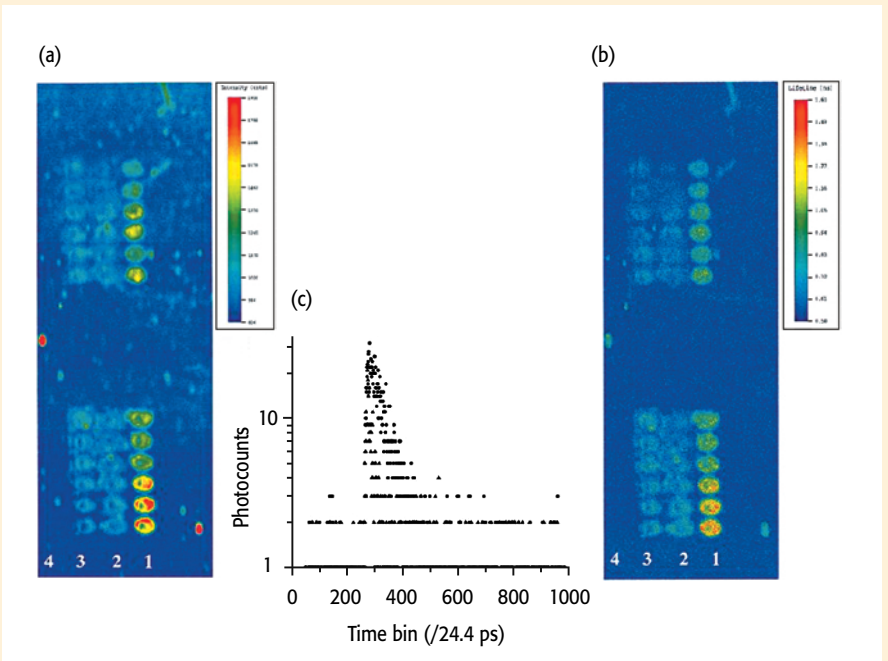

Figure 7. (a) Fluorescence intensity image and (b) lifetime image of two 4 × 6 DNA microarrays on modified PMMA slides. Columns in each array represent a (1) fully matched duplex, (2) a three-base mismatch, (3) a single-base mismatch, and (4) a complete mismatch. (c) Decay profiles for background and fluorescence from hybridization spot of array. Reprinted with permission from reference 10.

length by accumulating more spectral information in a band pair (see Figure 4). After the MLE analysis and base-shift correction was complete, it was found that the two-dye/two-lane format demonstrated a read length of 670 bases with an accuracy of 99.7%, and the single-dye/four-lane read accuracy was 95.7%. The reduction in errors using lifetime patterning was a consequence of increased information content in the electrophoretic bands experiencing poor electrophoretic resolution.

Using phase-resolved methods for lifetime analysis in DNA sequencing, McGown and coworkers demonstrated four-dye sequencing in one capillary (9). The researchers used a multiharmonic, Fourier transform modulation instrument (MHF) to extract the fluorescence lifetime in the frequency domain, thereby collecting an entire frequency response that allowed the analysis of multiexponential decays. Two NLLS base-calling methods were compared, recovering lifetimes for each peak to directly identify the base or recovering lifetime-resolved electropherograms for each base from the mixture of sequencing products.

The researchers investigated two sets of dyes in their measurements. One set was excited at 488 nm and the second set at 514 nm. Both sets of dyes were attached to an M13-forward primer for sequencing a pGEM-3Zf (+) ds-template.

The fluorescence lifetime instrument was interfaced directly to a Beckman Coulter (Fullerton, CA) P/ACE capillary electrophoresis (CE) system that was equipped with a CE–mass spectrometry interface to provide an external power supply for coupling to the MHF. An argon laser set at either 488 or 514 nm was used for excitation, and appropriate filters reduced the contribution from scattered laser light that was used for the lifetime reference. A cross-correlation frequency, where the gain of the detector is modulated at a frequency offset from that of the modulated excitation, of 10 Hz was used, which generated 10 phase-modulation measurements per second for on-the-

fly lifetime measurements. Cross-correlation detection allows the rejection of harmonics and other sources of noise. Ten consecutive measurements were averaged before data analysis to yield one lifetime measurement per second.

Two methods were used to analyze the lifetime sequencing information provided by the dynamic MHF. Using a one-component NLLS, bases were directly identified by calculating a lifetime and compared with predetermined lifetime values obtained from single-base tracts run under identical conditions. The second method involved using the NLLS analysis of on-the-fly lifetime data, in which lifetime components in the fitting models were obtained from prior sequencing of individual tracts and from which the lifetime-resolved electropherograms for each terminal base were obtained. Then, the recovered fractional intensity of each calculated lifetime component at each data point was multiplied by the total intensity at that point to reconstruct the electropherogram for each of the individual bases in the mixture.

The analysis of the dye set absorbing at 514 nm indicated that because of the low fluorescence of one dye, the set could not be used for a four-decay experiment. However, analysis of a two-dye experiment in this wavelength region was performed, and a read length of 304 bases from base 16 to 320 of the primer-annealing site was found. Using the direct method of recovering individual lifetimes, researchers achieved a 94% read accuracy, with most of the errors attributed to poor electrophoretic resolution. The identification also was performed using the lifetime-resolved intensity electropherograms and gave one error, which was attributed to an enzymatic abnormality, thus producing a read accuracy >99% for the same read length (304 bases).

A set of four 488-nm dyes including Cy 3, fluorescein-dTMR, rhodamine green, and BODIPY-FL with lifetimes of 0.9, 2.5, 2.9, and 3.5 ns, respectively, were evaluated for four-decay sequencing (see Figure 5). Sequential injections of each terminal base tract were analyzed via capillary gel electrophoresis, with a predetermined delay time between injection of each tract to adjust for mobility differences between the dyes. A read length of 179 bases was achieved with an accuracy of 96% (eight errors), which was determined by direct lifetime identification of the peaks. The NLLS analysis of the four-component run, when the lifetime values were set to predetermined values, was unsuccessful because of data analysis limitations.

Lifetime analysis of DNA also can be extended into the area of DNA microarrays for multiplexed detection. Many applications require screening of multiple probes that hybridize to one target tethered to a substrate, thereby providing different signals for varying levels of hybridization (differential expression assays) and reporting on the relative abundance of particular genes.

Soper and coworkers implemented an assay using time-resolved near-infrared (NIR) fluorescence to monitor signatures from DNA microarrays on glass, poly(methylmethacrylate) (PMMA), and poly-L-lysine substrates (10). The use of NIR analysis minimized the amount of background because few molecules exhibit fluorescence in this region and because the NIR method required simple instrumentation for time-correlated, single-photon counting (TCSPC).

NIR TCSPC measurements were made with an in-house-built device consisting of a 780-nm pulsed diode laser, a TCSPC PC-board, and a single-photon avalanche diode configured in an epi-illumination format using a mounting cube and lens tubes. The entire detector was mounted on an *x–y* microtranslational stage controlled by stepper motors interfaced to a PC. The step resolution of the scanner was 12.7 μm with a scan distance of 4 cm in both the *x* and *y* coordinates. The scanner would take one step then acquire

data for a software-selected integration time of 10 ms to 10 s. The data acquisition software recorded the position of the scanning head streaming data (both intensity and time-resolved) to the hard drive and providing real-time visualization of the fluorescence images. The controlling software included data analysis functions, which could display a two-dimensional image of both the lifetime and the fluorescence intensity along one horizontal or vertical line selected by a pair of cursors on the two-dimensional image. The fluorescence decay profiles were analyzed using MLE (see Equation 2).

Because low background levels for arrays are critical to increase the signal-to-noise ratio to interrogate the low loading levels of material, three types of substrates were investigated for their scattering and autofluorescence properties at 488- and 780-nm excitation. Poly-L-lysine, a substrate used for DNA microarrays because of its high binding affinity for DNA, yielded the highest background in both wavelength regions. Glass had a lower background in the visible region but generated a higher background compared with PMMA in the NIR region (see Figure 6). The time-dependent fluorescence profiles of glass and poly-L-lysine gave rise to a large, flat background believed to be caused by a long-lived luminescent species present in the slides. This background was absent in the case of PMMA.

PMMA was modified by attaching a diamine through the formation of an amide bond to the surface, followed by the attachment of the amino-modified oligonucleotide through the use of a glutaric dialdehyde cross-linking agent. After the oligonucleotides were attached, residual-free aldehyde groups of the cross-linker were capped with ethanol amine to prevent nonspecific adsorption of the target oligonucleotide to the substrate. The surface concentration of a 35-mer DNA was 400 molecules/μm^2, determined through the use of phosphorus-32–labeled oligonucleotides and scintillation counting.

For the hybridization assays, a 100-nM, IRD 800-labeled complementary target in a buffer solution was placed over the array and allowed to react for 30 min in the dark at 30 °C in a humidified chamber. The resulting intensity image of the array using a full-complement, one-base mismatch, three-base mismatch, and fully mismatched duplex confirmed that the assay could distinguish between duplex mismatches and demonstrated minimal nonspecific adsorption (see Figure 7). Compared with the intensity image of the array, the lifetime image showed fewer imperfections arising from scattering centers on the PMMA surface. The limit of detection found was 0.38 molecules/μm^2 but could be reduced

10-fold with the use of time-gated detection, which effectively discriminated the scattered photons from the fluorescence signal.

Conclusion

The use of fluorescence lifetime for the detection and identification of DNA in sequencing and microarray formats shows great promise in terms of adding more information content to fluorescence data. In addition, coupling lifetime identification protocols with spectral (color) discrimination can significantly enhance multiplexing capabilities. The development of more dye sets appropriate for lifetime methods possessing higher fluorescence quantum yields and uniform electrophoretic mobility within the set will improve the data analysis. Other analysis methods for lifetime identification also are being studied to determine whether improvements can be implemented in the calculation and recovery of lifetimes in complex data sets such as maximum entropy techniques.

Acknowledgment

The authors would like to thank the National Institutes of Health (NHGRI, HG01499-05) for partial financial support of this work.

References

1. J.C. Venter et al., *Science* **291** (5507),1304–1351 (2001).
2. The Human Genome Consortium, *Nature* **409**(6822), 860–921(2001).
3. B.B. Rosenblum, L.G. Lee, S.L. Spurgeon, S.H. Khan, S.M. Menchen, C.R. Heiner, and S.M. Chen, *Nucleic Acids Research* **25,** 4500–5404 (1997).
4. J.R. Lakowicz, "Data Analysis," in *Principles of Fluorescence Spectroscopy* (Kluwer Academic/ Plenum Publishers, New York, NY, 1999).
5. P. Hall and B. Selinger, *J. Phys. Chem.* **85,** 2941–2946 (1981).
6. S.A. Soper and B.L. Legendre, *Appl. Spectrosc.* **48,** 400–405 (1994).
7. U. Lieberwirth, J. Arden-Jacob, K.H. Drexhage, D.P. Herten, R. Müller, M. Neumann, A. Schulz, S. Siebert, G. Sagner, S. Klingel, M. Sauer, and J. Wolfrum, *Anal. Chem.* **70**(22), 4771–4779 (1998).
8. S.J. Lassiter, W. Stryjewski, B.L. Legendre, Jr., R. Erdmann, M. Wahl, J. Wurm, R. Peterson, L. Middendorf, and S.A. Soper, *Anal. Chem.* **72**(21), 5373–5382 (2000).
9. H. He and L.B. McGown, *Anal. Chem.* **72**(24), 5865–5873 (2000).
10. E. Waddell, Y. Wang, W. Stryjewski, S. McWhorter, A.C. Henry, D. Evans, R.L. McCarley, and S.A. Soper, *Anal. Chem.* **72**(24), 5907–5917 (2000). ■

Suzanne J. Lassiter is a graduate student, **Wieslaw J. Stryjewski** is a research associate, **Yun Wang** is a graduate student, and **Steven A. Soper*** is a professor in the Department of Chemistry, Louisiana State University, Baton Rouge, LA 70803-1804, (225) 578-1527, fax (225) 578-3458, e-mail steve.soper@chem.lsu.edu.

*To whom all correspondence should be addressed.